Abaqus user element for an accurate modeling of adhesive joints on coarse meshes

S. Joannès[*,**], J. Renard[**]

* CEMCAT, Parc Universitaire et Technologique,
Rue Léonard de Vinci, 53810 Changé, France
** Centre des Matériaux, Mines de Paris, ParisTech, CNRS UMR 7633 BP 87,
91003 Evry Cedex, France

Abstract: This work is concerned with the Abaqus implementation of a suitable CAE methodology to get the most benefits of structural adhesive bonding. In this study, we are interested in cohesive debonding where the adhesive thickness and its non-linear behavior are of major importance. When subjected to loading, significant stress field gradients may develop around outer edges of the joint. Because such regions are sites for failure initiation, a specific mesh refinement is needed. Using SIMULIA solutions, an efficient discretization strategy, inspired by the p-FEM, is suggested and is implemented as an Abaqus user element. Balancing the accuracy and the calculation time, in full-scale simulations, it is then possible to capture edge effects and damage initiation. As the approach is suggested to be used in real applications, a validation example has been chosen to show the suitability of the methodology on coarse meshes.

Keywords: Structural adhesive bonding, p-FEM, UEL subroutine, scripting.

1. Introduction

Designing safer, lighter and cleaner cars: that is the challenge to take up by constructors and parts manufacturers at the dawn of the 21st century. In addition to the use of new materials, the development of lightweight structures needs efficient joining methods. In recent years, structural adhesive bonding has proven to be highly successful and has become a popular joining technique for the transportation industry (Fays, 2003). Unlike bolted or riveted joints, adhesive bonding offer a continuum connection and has an extremely broad range of applications. It is nevertheless true that the development of structural adhesive bonding is hindered by several difficulties. For example, the determination of the load-carrying capacity of a bonded structure requires the analysis of the stress state in a very thin layer which exhibits stress fields gradients.

Indeed, in structural design, it is known for a long time that certain geometries like corners, edges or notches can cause harmful stresses. It's exactly the same for adhesive bonded joints in which geometrical characteristics change abruptly. That's why significant stress field gradients may develop around outer edges of the joint (edge effects). Because such regions are sites for failure initiation, a specific analysis is needed. For the most elementary geometric assemblies, like a single lap joint, analytical approaches seem to be well adapted (Adams, 1992), (Bigwood, 1990).

However, in the case of more complex geometrical configurations, it becomes impossible to describe the stress state analytically; it is then necessary to use numerical methods (Dean, 2001). Except for simplest geometries, capturing edge effects requires exploiting all the potential of the finite element method (Zienkiewicz, 2005).

Among SIMULIA solutions, Abaqus offers a library of elements to model behavior of adhesive joints. For situations where the integrity and strength of interfaces may be of interest, it is possible to use elements defined with zero thickness. Indeed, Cohesive Zone Modeling (CZM) (Chaboche, 2001), introduced at the end of 1980’s in most finite element codes, considers generally that the failure of an adhesive bond occurs at the interface between the adhesive and the adherends (adhesive or interfacial failure) rather than within the adhesive material (cohesive failure); see Figure 1. The CZM approach would treat the adhesive layer as an idealized interfacial surface material consisting of an upper and lower surface connected by a continuous distribution of normal and tangential disconnected springs. The assumption here is that if the thickness of the adhesive layer is small (compared to the length of the joint) the stress distribution through the thickness of the adhesive layer is negligible. This can be stated mathematically as: as the limit of the thickness tends to zero, the tractions at the upper and lower interfaces must be equal. This leads to the simplification that the tractions acting in the springs are uniform across the thickness. This assumption of zero thickness is not relevant when a crack propagates in the bulk polymer which constitutes the adhesive. In that case, taking into account the joint thickness and the non-linear constitutive behavior of the adhesive polymer are of major importance. For the continuation of this study, we are only interested in this last case with cohesive debonding.

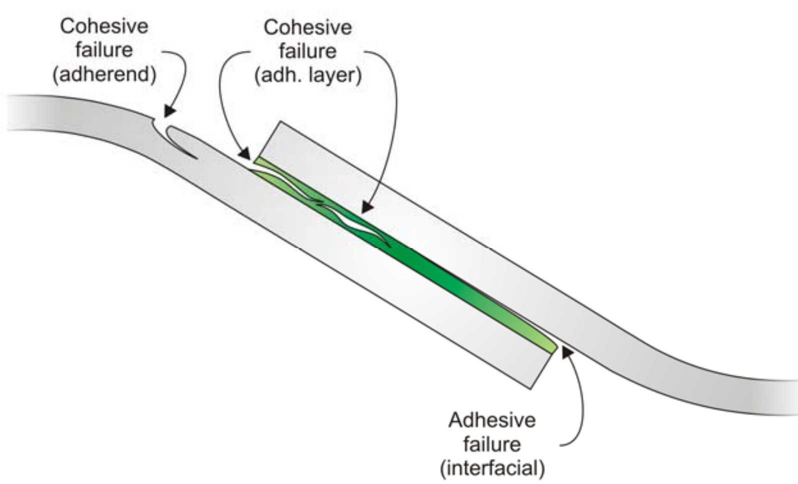

Figure 1. Fracture types of an adhesive joint.

Some specific elements, provided by Abaqus, can be used to model finite-thickness adhesives. The implementation of the conventional material models for cohesive elements is based on certain assumptions regarding the state of the deformation in the cohesive layer (Abaqus, 2006). Indeed, for those elements, it is assumed that the cohesive layer is subjected to only one direct component of strain, which is the through-thickness strain and to transverse shear strain components. The above kinematics assumptions are appropriate in situations where a relatively thin and compliant layer of adhesive bonds two relatively rigid (compared to the adhesive) parts. Moreover, these assumptions can be accepted inside the cohesive layer but not around its outer edges where complicated 3D stress could appear with significant gradients. Then, to capture edge-effects, it is necessary to use a very fine mesh in the regions of such transition zones. Balancing the accuracy and the calculation time, discretization has to be considered carefully, especially for full-scale structure simulations. Classical refinement techniques are time consuming and are not well adapted to industrial applications; Economic advantage requires a reduction of data preparation.

In this context, the aim of the work presented in this paper was the development of an efficient discretization strategy inspired by the p-FEM, and the extent of the Abaqus adhesive joints library models for industrial applications with coarse meshes.

2. User elements family based on the p-FEM

Numerical methods presented above require treating the adhesive bonded joints in a singular way (specific refinement). In the work presented in this paper, we suggest an alternative methodology which makes it possible to estimate the resistance of the adhesive bonded joint while preserving a “global” structural approach and classical numerical tools. Those two points are really key requirements for industrial applications. For this purpose, we exploit the potential of the p-version of the finite element method (p-FEM) which is based on hierarchical interpolation functions (Babuška, 1991).

2.1 A short introduction to the p-FEM and the hierarchical concept

In the finite element method, the error of approximation mainly depends on two parameters: the finite element mesh and the polynomial degree of elements. The size of the largest element in the model is generally denoted by “h”. It is obvious that errors of approximation decreased as h decreased. When the coarse mesh elements are broken into smaller elements, we speak about h-refinement. An alternative method, known as p-refinement controls the error of approximation by increasing the degree “p” of polynomial interpolation functions. We should note that with p-refinement, it is convenient to decrease the error of approximation still using the same coarse mesh elements. High order finite element methods have shown to be efficient in various applications and are gaining popularity in industry. The p-version of the finite element method is also associated with the hierarchical concept. Indeed, with the h-refinement method, a serious drawback exists: when element refinement is made, totally new interpolation functions have to be generated. In the hierarchic case, all lower order interpolation functions are contained in the higher order basis.

As the aim of this paper is not to describe exhaustively the p-FEM, we will only focus on the general concept. More information on the p-FEM and hierarchical approach can be found in (Peano, 1975), (Babuška, 1991), (Cugnon, 2000) and (Düster, 2001). Let's begin with the classical Lagrange interpolation and assume that in local (or element) coordinate system, we desire to define a quantity u^e by interpolating in space given values U^e. In a one-dimensional space, the element interpolation is given by Equation 1 with a set of interpolation functions N^e.

$$u^e(\xi) = \left[N^e(\xi)\right]\left\{U^e\right\} \tag{1}$$

Using the well known Lagrange interpolation, it is possible to define a linear interpolation between two nodes (Equation 2).

$$\begin{aligned} N_i^e(\xi) &= \prod_{\substack{j=1 \\ j\neq i}}^{2} \frac{(\xi - \xi_j)}{(\xi_i - \xi_j)} \\ \left[N^e\right] &= \left[\frac{1}{2}(1-\xi) \quad \frac{1}{2}(1+\xi)\right] \end{aligned} \tag{2}$$

By adding a third (center) node, the same technique can be used to obtain a quadratic interpolation (Equation 3).

$$\left[N^e\right] = \left[\frac{1}{2}(-\xi)(1-\xi) \quad \frac{1}{2}(\xi)(1+\xi) \quad 1-\xi^2\right] \tag{3}$$

Up to this point, with the Lagrange approach, if we desired to increase the interpolation order, we need to define totally new shape functions. With the hierarchic approach, to get new functions, we simply add some terms to the old functions. Thus, we add some "internal" interpolation functions, i.e. edge functions N_{A}^e, to nodal shape functions N_{N}^e (Equation 4).

$$\left[N^e\right] = \left[N_N^e \quad N_A^e\right] \tag{4}$$

As the element square matrix will always involve an integral of the product of the derivatives of the interpolation functions, hierarchical functions are based on orthogonal polynomials. That's why p-FEM is generally implemented using Legendre polynomials defined by Equation 5 called Rodrigues formula.

$$\begin{aligned} &\forall x \in [-1;1],\ \forall n \in \mathrm{N} / n \geq 2, \\ &L_n(x) = \frac{1}{2^n n!}\left[\frac{d^n}{dx^n}\left(x^2-1\right)^n\right] \end{aligned} \tag{5}$$

In the one-dimensional case, to obtain a $p \geq 2$ order of interpolation using the hierarchical approach, we can use Equation 6 and Equation 7.

$$\left[N^e\right] = \left\lfloor \frac{1}{2}(1-\xi) \quad \frac{1}{2}(1+\xi) \quad N^e_{\mathrm{A1}\{p\}}(\xi) \right\rfloor \tag{6}$$

$$\begin{aligned} &\forall p \in \mathrm{N} \,/\, p \geq 2, \\ &\qquad N^e_{\mathrm{A1}\{p\}}(\xi) = \frac{1}{\sqrt{4p-2}}\left[L_p(\xi) - L_{p-2}(\xi)\right] \end{aligned} \tag{7}$$

In the same way, it is easy to construct hierarchical interpolation functions for 2D and 3D elements. As we said earlier, for a one-dimensional element, we have nodal and edge interpolation functions: nodal functions are defined by Lagrange polynomials and edge functions by Legendre polynomials. For a two-dimensional element, we must add face functions N^e_{F} (Equation 8) and for a three-dimensional element internal functions N^e_{I} (Equation 9). Face functions and internal functions are respectively defined by a combination of (ξ, η) interpolations and (ξ, η, ζ) interpolations.

$$\left[N^e\right] = \left[N^e_{\mathrm{N}} \quad N^e_{\mathrm{A}} \quad N^e_{\mathrm{F}}\right] \tag{8}$$

$$\left[N^e\right] = \left[N^e_{\mathrm{N}} \quad N^e_{\mathrm{A}} \quad N^e_{\mathrm{F}} \quad N^e_{\mathrm{I}}\right] \tag{9}$$

The Figure 2 gives a graphical representation of a bilinear nodal interpolation associated with a 2nd order hierarchical interpolation for a four nodes 2D element. We can see the representation of four nodal functions, four edge functions and one face function. For the same element, the Figure 3 gives a graphical representation in the case of a 3rd order of interpolation.

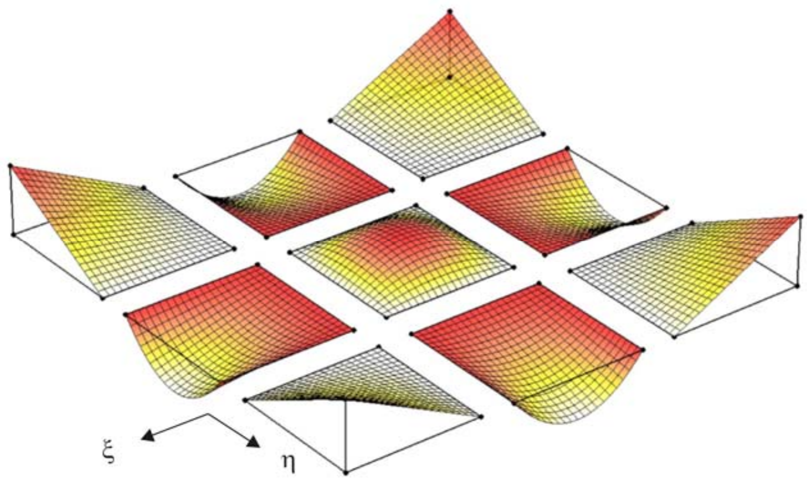

Figure 2. 2D, four nodes element, 2nd order interpolation: graphical representation of four nodal functions (bilinear), four edge functions and one face function.

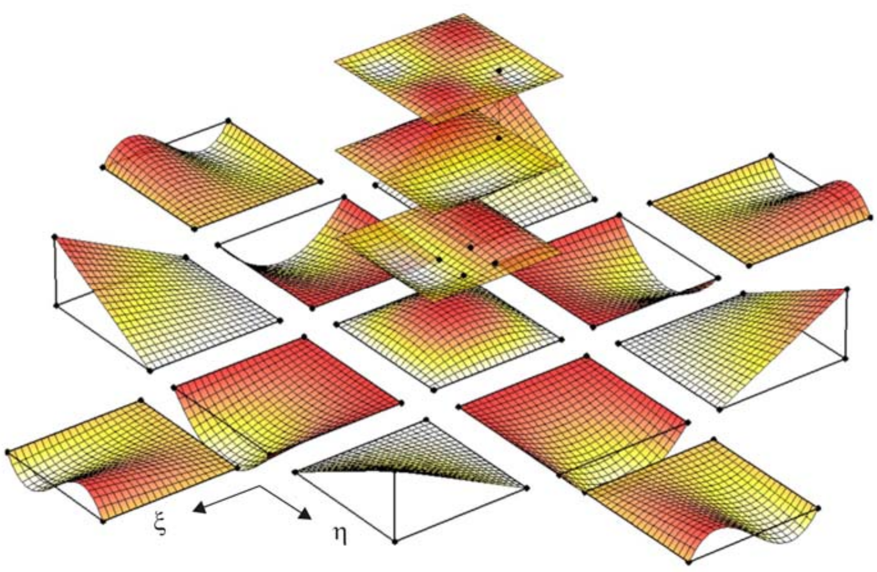

Figure 3. 2D, four nodes element, 3rd order interpolation: graphical representation of a four nodal functions (bilinear), four edge functions of degree two, four edge functions of degree 3 and four face functions (degree 2x2, 3x2, 2x3, 3x3).

Up to now, we have shown “isotropic” increase of the element order. With the hierarchical approach presented above, it is possible to adopt an “anisotropic” p-refinement of the element (Düster, 2001). Indeed, we can define independent degrees of interpolation for each space directions. An example can be seen on Figure 4.

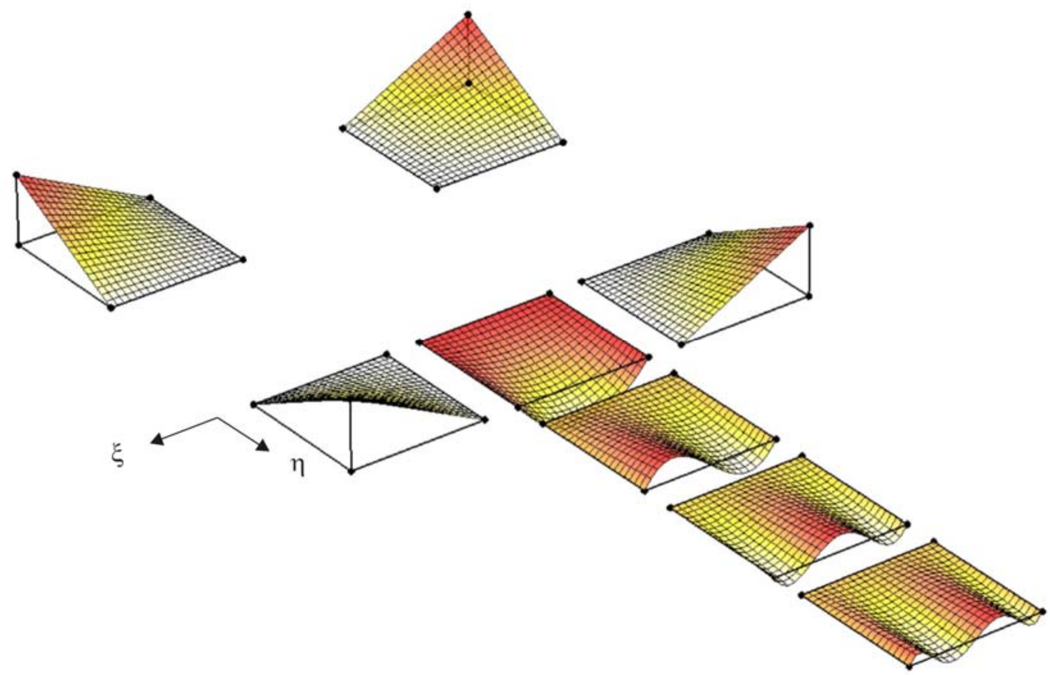

Figure 4. 2D, four nodes element, 5th order interpolation for one edge of the element.

2.2 A specific formulation for capturing edge effects

Capture the strong variations of the solution in the vicinity of the ends of the joint… For this goal and to introduce more easily the formulation suggested, let us consider a one-dimensional “academic” problem: an “ideal” straight bar composed of a linearly elastic material and subjected to an axial tension load as depicted in Figure 5. The solution $x \mapsto u(x)$ describes the displacement of the bar in x direction. The bar is loaded by a force per unit length $x \mapsto f(x)$ in the bar cross-sectional direction and a punctual load F for $x = \ell$. The Young modulus is denoted E, the cross-sectional area A, the density ρ and the bar length ℓ. The problem is modeled by Equation 10 with a clamped end for $x = 0$.

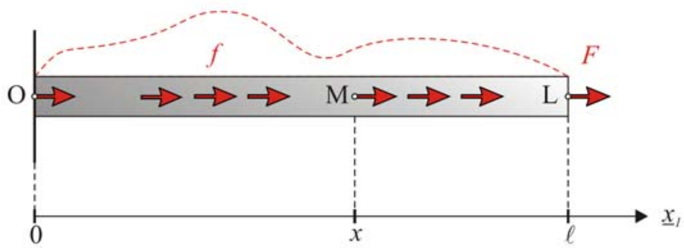

Figure 5. The academic bar problem: a simple one dimensional case to introduce the formulation of the user element family.

$$\begin{cases} EA\dfrac{d^2u}{dx^2}+\rho A f=0 \quad \forall \mathrm{M}\in\Omega \\ u(\mathrm{O})=0 \qquad\qquad \text{for M=O,}(x=0) \\ \left[\dfrac{du}{dx}\right]_L=\dfrac{F}{EA} \qquad \text{for M=L,}(x=\ell) \end{cases} \tag{10}$$

Imposing a solution with a very strong variation, we study the efficiency of the hierarchical formulation according to the selected degree. In Figure 6 the approximation for a degree 8 hierarchical interpolation is plotted together with the exact solution of the problem (Equation 11).

$$u_{ex}(x)=x^{50} \tag{11}$$

At first sight, with a single element of degree 8, we manage with difficulty to approach the exact solution of “degree 50”. We can of course continue to increase the order of interpolation or refine the mesh but that would be to the detriment of the computing time and the aims of this work. It also should be noted that the oscillations observed do not facilitate the research of the result. If the integration of the stiffness matrix and the elementary vectors is accessible here analytically, that is seldom the case for most complex problems. When the element is deformed, the geometrical transformation is not linear anymore and the Jacobian matrix is a sophisticated polynomial function. Explicit integration becomes impossible and it is then necessary to use numerical integration techniques.

In this paper, we suggested a way to improve the approximation and capture edge effects without increase the order of interpolation or refine the mesh (Joannès, 2007).

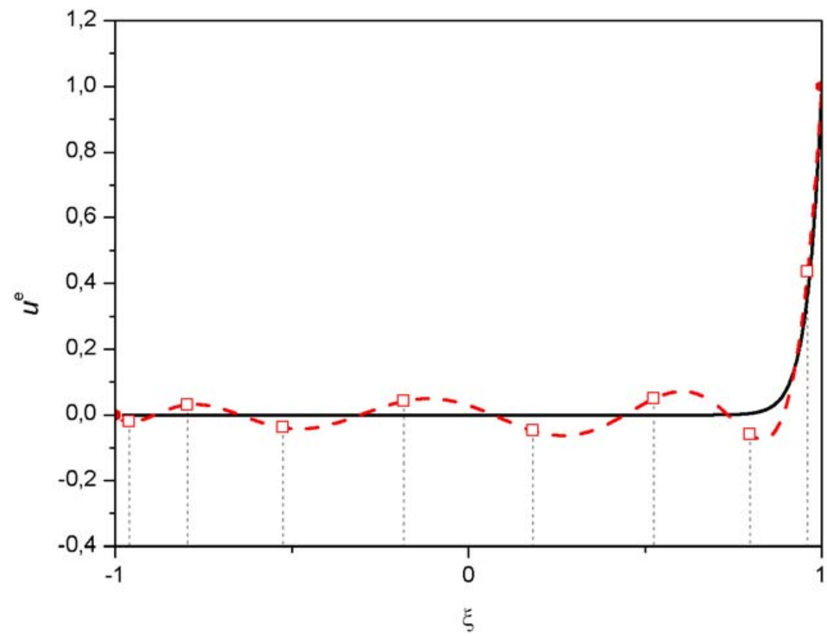

Figure 6. Approximation of the exact solution by a degree 8 hierarchical interpolation. Integration points are represented by square symbols.

In order to attenuate oscillations phenomena and better capturing edge effects, we should optimize the element previously described and "distend" the solution near the element boundaries. We choose to supplement the linear geometrical interpolation (Equation 12) by a suitable cubic interpolation. It is essential that this new function don't modify the values "on", but "near" the boundaries.

$$[P^e] = \left[\frac{1}{2}(1-\xi) \quad \frac{1}{2}(1+\xi) \right] \tag{12}$$

The "distending" parameter is denoted δ and we define a new function $\xi,\delta \mapsto A(\xi,\delta)$ which is the cubic additional polynomial (Equation 13).

$$[P^e] = \left[\frac{1}{2}(1-A(\xi,\delta)) \quad \frac{1}{2}(1+A(\xi,\delta)) \right] \tag{13}$$

If $\delta = 1$ there is no additional transformation but when $\delta \rightarrow 0$ the distending becomes maximal. The new geometrical interpolation functions are no longer identical to the nodal interpolation of the solution, except if $\delta = 1$. We choose to preserve a pseudo-parametric or sub-parametric element and the additional transformation intervenes only when $p \geq 3$.

While preserving the degree 8, this additional geometrical transformation enables us to find a value of δ for which the error of approximation becomes minimal (Figure 7).

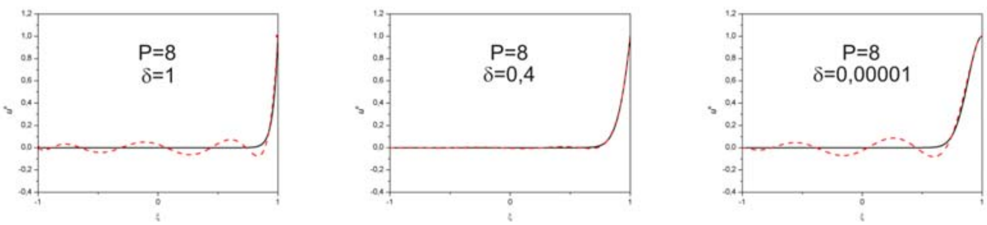

Figure 7. Approximation of the exact solution by a degree 8 hierarchical interpolation and applying a geometrical "distending" of the solution near the boundaries of the element.

3. A suitable CAE methodology

The family of elements discuss previously is implemented as an Abaqus user element and is associated with a dedicated pre- and post-processing (Abaqus Python scripts). With this methodology, it is possible to preserve "industrial" meshes with a reasonable description of the adhesive joint behavior while ensuring a total compatibility with Abaqus code. This tool takes the form of a user subroutine which allows "enriching" a portion of the mesh, for example the adhesive layer, with a hierarchical formulation. The subroutine is organized in a modular way and allows managing the elementary matrix and vectors construction. Since we act only on specific zones, the global assembly as well as the resolution of the problem is done by Abaqus. In complement to the UEL subroutine, we have developed pre- and post-processing capabilities. The purpose of the pre-processing is to transform the input file describing the problem (mesh, boundary conditions and loads) in order to substitute the standard elements of the adhesive zone by elements with hierarchical formulation. The program integrates a strategy of classification of the additional degrees of freedom particularly efficient: the enrichment of hierarchical elements is entirely controlled by the "edges" of the elements. Coupled with an error indicator, this choice makes it possible to consider automatic calculations.

Post-processing provides graphical information for Abaqus visualization module by representing the results obtained with hierarchical elements. Taken as a whole, the tool implemented represents about ten thousand lines of Fortran and Python codes with nearly two thirds devoted to the central subroutine (UEL). The implementation presented above allows considering three dimensional structural problems. It is based on a hexahedral element formulation, being able to vary the polynomial degree for the three local directions. The use of anisotropic interpolation leads to very efficient approximations.

3.1 Patch tests

The successful application of finite element analysis should always include a validation of the elements to be used and a validation of their implementation in a specific computer program. A single element test can show the effects of the element geometrical parameters such as convexity, aspect ratio or skewness. The patch test has been introduced as a complementary check for continuity intra- and inter-elements. It was developed from physical intuition and later written in mathematical forms. The concept is fairly simple: to be assured of convergence one must be able to exactly satisfy the state where the derivatives, in the governing integral statement, take on constant or zero values. Thus, the patch test provides a simple numerical way to verify that correct programming was achieved and that the element behaves as it should. We define a patch of elements to be a mesh where at least one node is completely surrounded by elements. Any node of this type is referred to as an interior node. The outer nodes are referred to as exterior nodes. The exterior nodes are utilized to introduce the essential boundary conditions and loads required by the test. The Figure 8 presents the patch meshes used for 2D and 3D user elements. In order to verify the transition between standard and user elements, exterior elements are CPE4 or C3D8 elements and share at least one node with user inner elements. By moving the central node, we have distorted user elements to see the effect that has on the numerical accuracy of the patch. With various interpolation configurations, we have applied rigid body modes, constant strain and constant stress state and controlled the accuracy of the patch response. For example, a rigid body displacement of the patch should not introduce strain nor stress change.

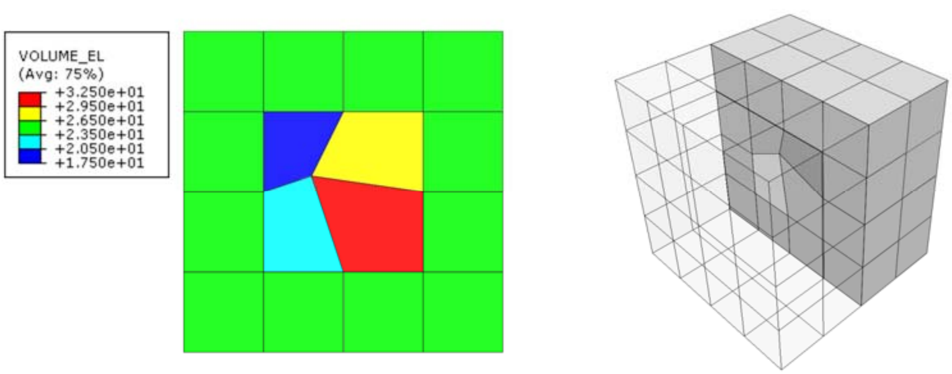

Figure 8. Patch meshes for 2D and 3D user elements tests.

3.2 2D validation example

Previous tests have validated the behavior of a family of user elements (2D and 3D) based on a hierarchical interpolation and implemented in Abaqus (Abaqus, 2006). The following paragraph highlights the relevance of the methodology for high stress gradients. The problem presented here is directly derived from the 2D patch-test: by the removal of four elements and the readjustment of the central node, we obtain a “L” shape. This configuration is particularly interesting from a numerical point of view since it induces a very strong gradient of stress. The model comprises twelve 2D elements with four geometrical nodes. The three central elements have elastic properties ten times higher than those of the peripheral elements. The test consists in imposing a uniform displacement on the higher border of the L, while immobilizing in a suitable way the base and the side (Figure 9). On the peripheral edges, the degree of interpolation is fixed (linear interpolation). For interior edges, the degree is free to evolve anisotropically. A “reference” mesh, comprising 2700 elements with linear interpolation (5642 degrees of freedom), makes it possible to assess the relevance of the hierarchical model which comprises only 378 degrees of freedom on the Figure 10 (with a maximum degree of four in that case). The Figure 10 confronts the results obtained for the shear stress field. We can note a very good correlation of the results, even in re-entrant corner zone while having here very little elements and a relatively weak interpolation degree (“only” four).

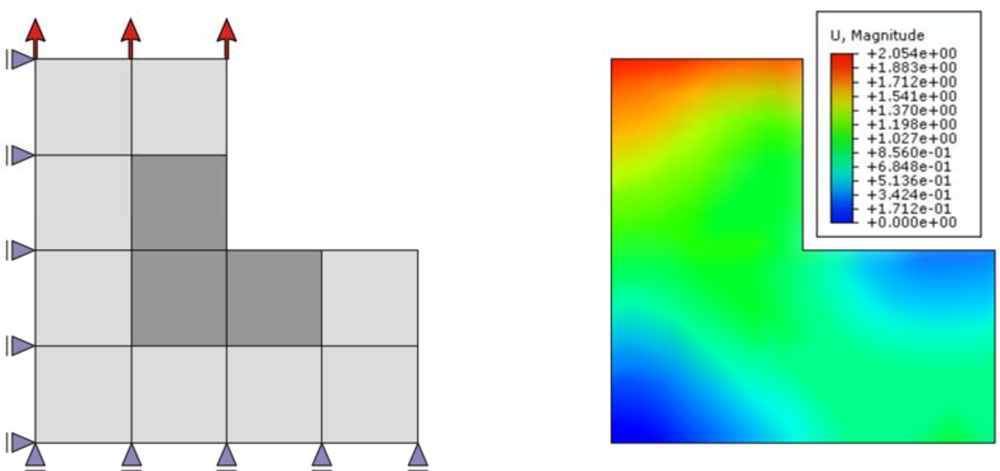

Figure 9. The “L” shape helps the numerical validation of the hierarchical interpolation with very strong gradients of stress. Representation of the boundary conditions and visualization of the displacement field (magnitude) induced.

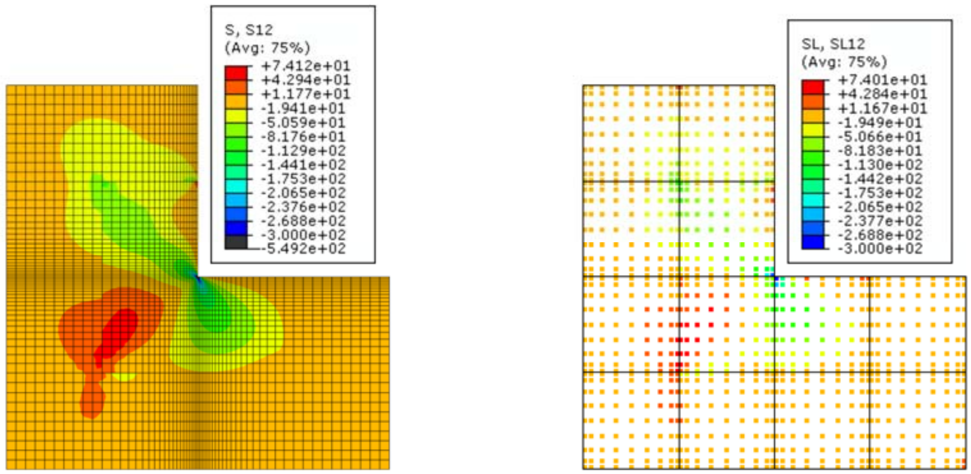

Figure 10. Confrontation of the results obtained on a benchmark model (left: 2700 bi-linear elements) and by a hierarchical approach (right: twelve user elements). The good correlation of these results shows the relevance of the hierarchical approach for capturing strong variations of the solution.

3.3 3D validation example

In addition to the 2D validation problem, we wished to work on three-dimensional subsystems representative of adhesive bonded joints. Three configurations were defined: single lap shear test (Figure 11), peeling test (Figure 12) and compression on tubes. For each one of these tests, we used the hierarchical approach combined with a non-linear anisotropic behavior dedicated to adhesive exhibiting high hydrostatic sensitivity (Joannès, 2007).

Starting from a conventional input file, the pre-processing replaces the standard elements of the targeted zones by user elements with hierarchical formulation. The interpolation compatibility on transition zones is assured. The initial degree is fixed beforehand but can evolve locally according to the need. This local adaptation could be obtained automatically by using an error indicator related to each edge. During this adaptation phase, it is important to use the simplest behavior model for the adhesive (linear elasticity). Once the desired precision reached, calculation can be launched with a non-linear and anisotropic behavior. The principal subroutine generates results files for nodal variables and integration points evaluation. Post-processing performs data conversions for the visualization module. It is then possible to display results within the adhesive bonded joint (Figure 12).

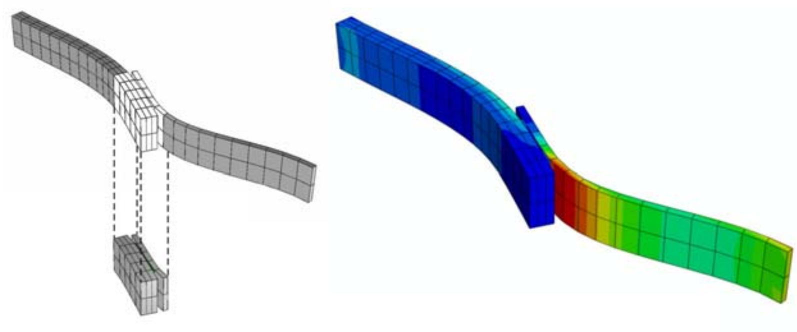

Figure 11. Single lap joint. Elements with standard formulation are replaced by elements with hierarchical formulation around the adhesive joint; the interpolation compatibility on the transition zone is assured.

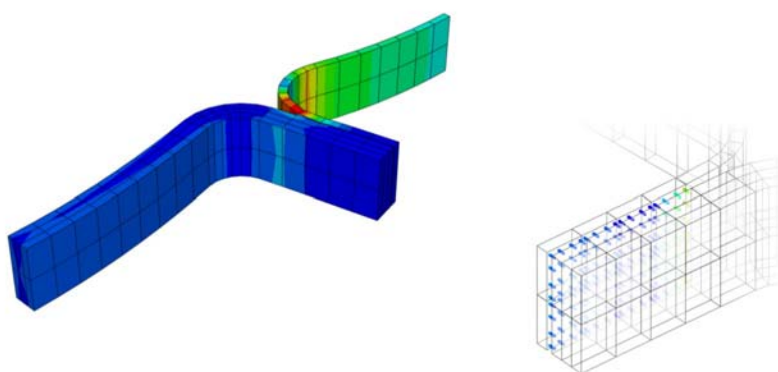

Figure 12. Peeling test. Post-processing performs data conversions for the visualization module. It is then possible to display results obtained by the hierarchical approach within the adhesive bonded joint.

4. Concluding remarks

The use of finite element methods allow the study of complex configurations. Nevertheless, the degree of accuracy is in direct correspondence with the number and the type of elements used. Very often, localized stresses in multi-materials structures impose the use of a great number of elements. Developments of the numerical analysis led to the emergence of specific tools which remain more or less applicable to the targeted industrial cases. A new approach, based on a hierarchical formulation, has been presented in this paper. This tool takes into account the localized phenomena governing the behavior of adhesive joints while guaranteeing compatibility with a coarser industrial modeling. This work brings an appropriate response to industrial constraints. Confrontations between experimental tests and numerical calculations are particularly encouraging. Finally, the modularity of the implementation allows its extension to other fields of applications such as detecting delamination on composites materials.

5. References

1. Abaqus/Standard, User's Manual, version 6.6, Hibbitt, Karlsson and Sorensen Inc, 2006.
2. Adams, R. D. and Mallick, V., “A method for the stress analysis of lap joints”, The Journal of Adhesion, vol. 38, no.3-4, pp. 199-217, 1992.
3. Babuška, I. and Szabó, B. A., “Finite element analysis”, John Wiley and Sons, 1991.
4. Besson, J., Cailletaud, G., Chaboche, J. L. and Forest, S., “Mécanique non linéaire des matériaux”, Hermès, 2001.
5. Bigwood, D. A. and Crocombe, A. D., “Non-linear adhesive bonded joint design analysis”, International Journal of Adhesion and Adhesives, vol. 10, no. 1, pp. 31-41, 1990.
6. Chaboche, J. L., Feyel, F. and Monerie, Y., “Interface Debonding Models: A viscous regularization with a limited rate dependency”, International Journal of Solids and Structures, vol. 38, no. 18, pp. 3127-3160, 2001.
7. Cugnon, F. “Automatisation des calculs éléments finis dans le cadre de la méthode-p”, Ph. D. Thesis, Université de Liège, Belgium, 2000.
8. Dean, G. D. and Crocker, L., “The Use of Finite Element Methods for Design with Adhesives”, Measurement Good Practice Guide, no. 48, National Physical Laboratory, UK, 2001.
9. Düster, A., “High order finite elements for three dimensional, thinwalled nonlinear continua”, Ph. D. Thesis, Technische Universität München, Germany, 2001.
10. Fays, S., “Adhesive Bonding Technology in the Automotive Industry”, Adhesion and Interface, vol. 4, no. 2, pp. 37-48, 2003.
11. Joannès, S., “Caractérisation mécanique et outil d’aide au dimensionnement des collages structuraux”, Ph. D. Thesis, Ecole Nationale Supérieure des Mines de Paris, ParisTech, France, 2007.
12. Peano, A. G., “Hierarchies of conforming finite elements”, Ph. D. Thesis, Washington University, St. Louis, USA, 1975.
13. Zienkiewicz, O. C., Taylor, R. L. and Zhu, J. Z., “The Finite Element Method, its basis & fundamentals”, Elsevier Butterworth-Heinemann, Sixth Edition, 2005.